Theoretical Study of Multidimensional Proton Tunnelling in Benzoic Acid Dimer

Marek J. Wójcik[*], Krzysztof Szczeponek and Marek Boczar

Faculty of Chemistry, Jagiellonian University, 30-060 Kraków, Ingardena 3, Poland
[*]Author to whom correspondence should be addressed. E-mail: wojcik@chemia.uj.edu.pl

Abstract: *Ab initio* B3LYP/6-311++G** calculations have been carried out for the benzoic acid dimer for the stable and saddle point structures. The energy barrier for the proton tunneling amounts to 6.5 kcal/mol. The normal mode frequencies have been computed including modes coupled to the proton tunneling mode. Two-dimensional model potentials, formed from symmetric mode coupling potential and squeezed double well potential, have been fitted to the calculated energy barrier, geometries and frequencies, and used to analyze proton dynamics. The calculated proton tunneling energy splitting in the vibrationally ground states of the low-frequency modes is ~230 cm^{-1}. The two-dimensional model PES predict monotonic increase of the tunneling splitting with the excitation of the planar modes. Depending of the sign of the coupling parameter out-of-plane modes can either suppress or promote the splittings.

Keywords: proton tunnelling, energy barrier, tunnelling splittings.

Introduction

The importance of proton tunneling in chemical and biological systems is well known, e.g. for the DNA base pairing, as discussed by Löwdin [1]. The phenomenon of potential barrier penetration plays an important role in many branches of physics: quantum field theory, fission of atomic nuclei, scanning tunneling microscopy and solid state physics [2]. Theoretical studies of proton tunneling require the knowledge of multi-dimensional potential energy surfaces (PES's) which are difficult to obtain from *ab initio* calculations, especially for electronically excited states. From the theoretical point of view proton transfer in the ground electronic state is more easily tractable. Extensive

experimental and theoretical studies have been reported for multidimensional proton tunneling in tropolone [3-13]. Vener et al. [10] studied theoretically multidimensional proton tunneling in tropolone by using adiabatic separation of variables. Smedarchina et al. [11] used the instanton approach to account for tunnelling splittings. Takada and Nakamura [12] on the base of high accuracy *ab initio* calculations proposed a model potential energy surface (PES) for the electronically ground $\widetilde{X}$ state and employed it to analyze the proton tunnelling dynamics. Wójcik et al. [13] reported the results of the high accuracy *ab initio* MO calculations of the potential energy surfaces in the excited Ã state of tropolone, and by fitting the two- and three-dimensional analytical model potentials to these surfaces and solving the multidimensional vibrational problems, interpreted the existing experimental data. Other systems for which tunnelling have been studied include malonaldehyde [14-17], formic acid [18], hydrogen-oxalate anion [16], substituted tropolone [19,20] and 5-methyl-9-hydroxyphenalenone (OH and OD) [21], methanol tetramer [22] and hydrogen carbonate dimer ion [23]. Recently a mixed quantum-classical approach has been used to study dynamics of hydrogen-bonded systems [24,25].

System which draws our attention in the present paper is benzoic acid dimer. It is present in the structure of the crystal [26-28]. Its proton transfer has been recently studied by inelastic neutron scattering by Plazanet et al. [29] and Fillaux et al. [30]. Vibrational spectra of benzoic acid have been reported in Refs. [31-32]. In this article we present the results of high accuracy *ab initio* MO and DFT calculations of the potential energy surfaces for the ground state of benzoic acid dimer in the stable and saddle point structures, and by fitting the two-dimensional analytical model potentials to these surfaces and solving the multidimensional vibrational problems, we predict the effects of excitations of the low-frequency in- and out-of-plane modes on the proton tunnelling splittings.

This paper is organized as follows. The results of our quantum chemical calculations for the ground state of benzoic acid dimer are presented in Sec. II. Model studies of the tunnelling are discussed in Sec. III. Concluding remarks are given in Sec. IV.

Quantum Chemical Calculations

We performed *ab initio* B3LYP/6-311++G** calculations for the ground state of benzoic acid dimer using the Gaussian 98 program package [33]. The calculations have been done in the Computer Center of Hokkaido University in Sapporo, Japan and the Department of Materials Chemistry, Uppsala University in Sweden. The calculations have been performed for the stable and the saddle point structures. The geometry of benzoic acid dimer in the stable and the saddle point structures, calculated by the B3LYP/6-311++G** method is shown in Fig. 1. Optimized geometry is summarized in Table 1. The complex is planar in the stable and the saddle point structures. The calculated values reproduce the experimental bond lengths and angles reasonably well. There are small discrepancies for C_1-O_2 and some C-C distances. Experimental C-H distances taken from Ref. [26] are only estimates. The angles are well reproduced except $O_2C_1C_2$. The influence of the saddle point structure on geometry in hydrogen-bonded cyclic structure is considerable.
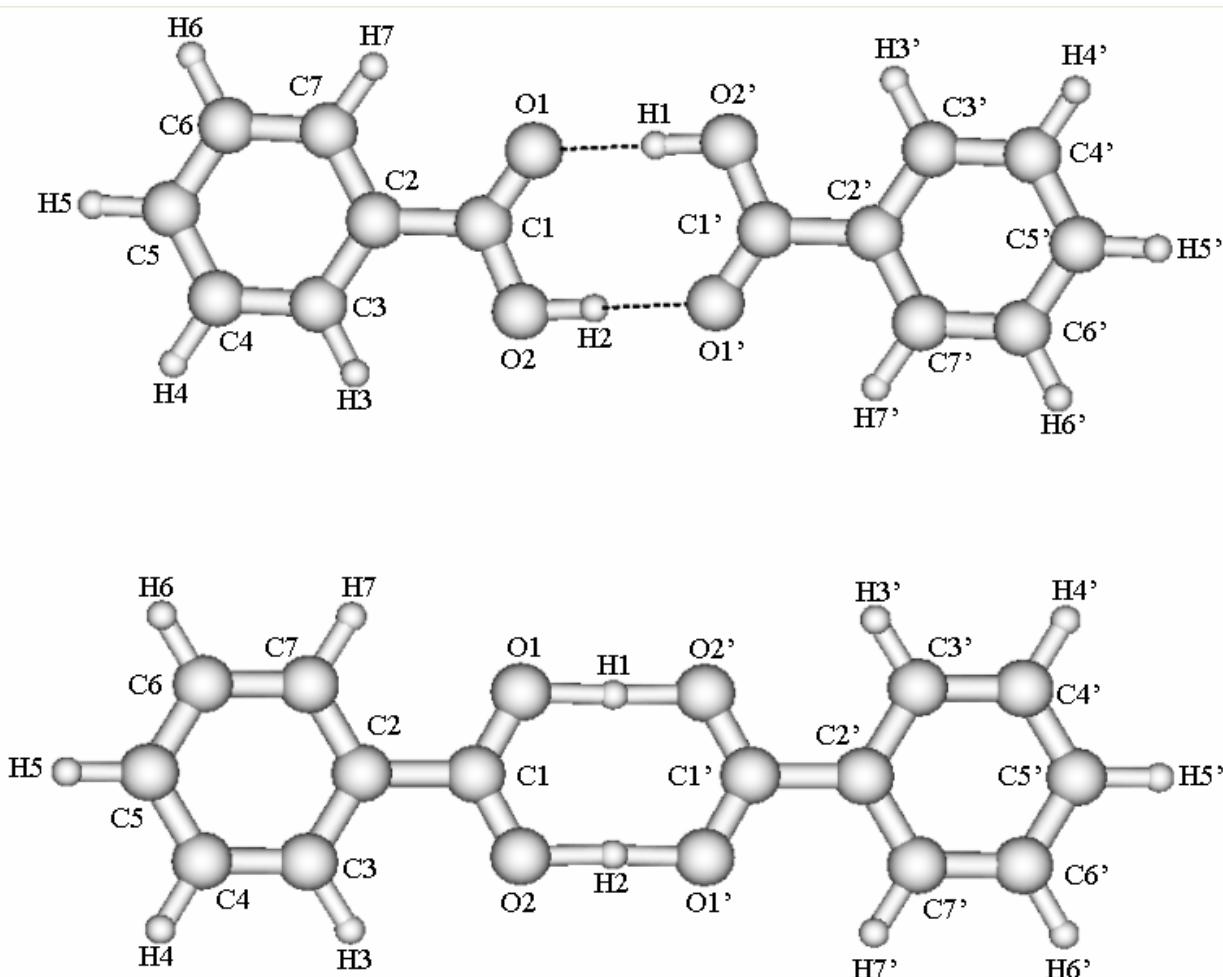
Figure 1. Benzoic acid in the stable and saddle point structures.

The calculated frequencies and symmetries of the normal modes at the stable and the saddle point structure are summarized in Table 2. The modes calculated by the B3LYP/6-311++G** method and used in the model calculations are pictured in Fig. 2. The frequencies have not been scaled. The agreement between experimental and calculated frequencies is generally good, especially in the low and medium-frequency regions. The calculated frequencies in the region of O-H and C-H stretchings are overestimated by about 100-150 cm^{-1} and the frequency of the O-H symmetric stretching mode v_{73} is overestimated by ~500 cm^{-1}. This is partly due to harmonic approximation and effects of intermolecular interactions on this mode in the crystal.

Table 1. Optimized geometries of the stable and saddle point structures of benzoic acid by the B3LYP/6-311++G** (DFT) method.

	Stable structure		Saddle point structure
	DFT	EXP.	DFT
Bond lengths (Å)			
$O_1 \cdots O_2'$	2,663	2,64[a]; 2,629[b]; 2,633[c]	2,410
$O_1 - H_1$	1,663	1,64[b]	1,205
$O_2 - H_2$	1,000	0,988[b]	1,205
$C_1 - O_1$	1,230	1,24[a]; 1,268[b]; 1,263[c]	1,272
$C_1 - O_2$	1,323	1,29[a]; 1,275[b]; 1,275[c]	1,271
$C_2 - C_1$	1,486	1,48[a]; 1,484[c]	1,486
$C_2 - C_3$	1,400	1,39[a]; 1,390[c]	1,400
$C_3 - C_4$	1,391	1,42[a]; 1,387[c]	1,391
$C_4 - C_5$	1,395	1,36[a]; 1,379[c]	1,395
$C_5 - C_6$	1,395	1,37[a]; 1,384[c]	1,395
$C_6 - C_7$	1,390	1,41[a]; 1,401[c]	1,391
$C_7 - C_2$	1,400	1,39[a]; 1,392[c]	1,400
$C_3 - H_3$	1,082	0,79[a]	1,082
$C_4 - H_4$	1,084	0,96[a]	1,084
$C_5 - H_5$	1,084	0,91[a]	1,084
$C_6 - H_6$	1,084	0,96[a]	1,084
$C_7 - H_7$	1,083	0,79[a]	1,082
Bond angles (°)			
$O_1 H_1 O_2'$	177,14		179,63
$C_1 O_1 H_1$	126,84		116,66
$C_1 O_2 H_2$	110,27		116,71
$O_1 C_1 O_2$	123,26	122[a]; 123,2[c]	123,78
$O_2 C_1 C_2$	114,50	118[a]; 119,9[c]	118,12
$C_2 C_1 O_1$	122,24	122[a]; 120,2[c]	118,11
$C_1 C_2 C_3$	121,40	122[a]; 118,0[c]	120,04
$C_3 C_2 C_7$	119,90	119[a]; 119,9[c]	119,92
$C_7 C_2 C_1$	118,70	119[a]; 118,8[c]	120,04
$C_2 C_3 C_4$	119,86	118[a]; 120,1[c]	119,94
$C_3 C_4 C_5$	120,02	123[a]; 119,9[c]	120,03
$C_4 C_5 C_6$	120,15	118[a]; 120,3[c]	120,16
$C_5 C_6 C_7$	119,98	122[a]; 119,7[c]	120,03
$C_6 C_7 C_2$	120,02	120[a]; 119,8[c]	119,94
$C_2 C_3 H_3$	119,48		119,11
$H_3 C_3 C_4$	120,66		120,95
$C_3 C_4 H_4$	119,85		119,89
$H_4 C_4 C_5$	120,07		120,08
$C_4 C_5 H_5$	119,91		119,92
$H_5 C_5 C_6$	119,94		119,92
$C_5 C_6 H_6$	120,09		120,08
$H_6 C_6 C_7$	119,93		119,89
$C_6 C_7 H_7$	121,12		120,95
$H_7 C_7 C_2$	118,86		119,12

[a] Ref. 26, [b] Ref. 27, [c] Ref. 28.

Table 2. Calculated normal mode frequencies for the stable and saddle point structures of benzoic acid by the B3LYP/6-311++G** (DFT) method.

No.	Symmetry	Frequency (cm⁻¹)		
		Stable structure	Saddle point structure	Literature Infrared
1	AU	22	22	25[b]
2	AU	33	35	35[b]
3	BG	41	17	41[b]
4	BU	60	75	71[b]
5	BG	64	62	79[b]
6	AU	87	79	94[a]
7	AG	106	120	110[b]
8	AG	114	201	127[b]
9	AU	172	174	146[a]
10	BG	179	177	
11	AG	259	294	
12	BU	283	363	
13	BU	389	385	
14	BG	414	413	
15	AU	415	415	
16	AG	423	588	
17	AU	446	448	421[a]
18	BG	448	451	
19	AG	512	529	
20	BU	546	723	491[a]
21	AG	632	632	
22	BU	632	631	615[a]
23	AG	669	729	
24	BU	679	698	669[a]
25	BG	694	699	
26	AU	696	697	687[a]
27	BG	707	680	
28	AU	724	729	711[a]
29	BG	804	788	
30	AG	804	824	
31	BU	816	866	767[a]
32	AU	831	838	813[a]
33	AU	866	865	
34	BG	866	865	856[a]
35	BG	886	1203	
36	BG	961	961	
37	AU	963	965	937[a]
38	AU	982	1327	960[a]
39	BG	1000	999	
40	AU	1000	999	974[a]
41	BG	1010	1009	998[a]
42	AU	1011	1009	
43	BU	1018	1015	1002[a]
44	AG	1018	1018	
45	BU	1046	1044	1027[a]
46	AG	1046	1047	
47	AG	1101	1101	
48	BU	1101	1101	1066[a]

Table 2. Continued.

No.	Symmetry	Frequency (cm^{-1})		
		Stable structure	Saddle point structure	Literature Infrared
49	BU	1146	1121	1027[a]
50	AG	1150	1173	
51	BU	1184	1184	1164[a]
52	AG	1184	1184	
53	BU	1198	1185	1185[a]
54	AG	1199	1202	
55	AG	1309	1436	1316[a]
56	BU	1317	1563	1322[a]
57	AG	1344	1337	
58	BU	1346	1338	1297[a]
59	AG	1350	1350	
60	BU	1350	1350	1380[a]
61	BU	1453	1449	1430[a]
62	AG	1474	1477	
63	BU	1480	1478	1456[a]
64	AG	1486	1697	
65	AG	1524	1523	
66	BU	1524	1526	1496[a]
67	BU	1620	1616	1590[a]
68	AG	1621	1614	
69	BU	1643	1642	1606[a]
70	AG	1643	1641	
71	AG	1686	1696	1699[a]
72	BU	1731	1690	1738[a]
73	AG	3102	1194 i	2605[a]
74	BU	3166	3167	3012[a]
75	AG	3166	3167	
76	BU	3179	3179	3041[a]
77	AG	3179	3179	
78	BU	3187	3189	3068[a]
79	AG	3188	3189	
80	BU	3197	1216	3312[a]
81	AG	3203	3206	
82	BU	3203	3206	3079[a]
83	BU	3210	3207	3098[a]
84	AG	3210	3207	

[a] Ref. 30, [b] Ref. 31.

In Table 3 we present the calculated energies and potential barriers. The energy barrier for the proton transfer amounts to 6.497 kcal/mol, no ZPE and only 1.867 kcal/mol, with ZPE.
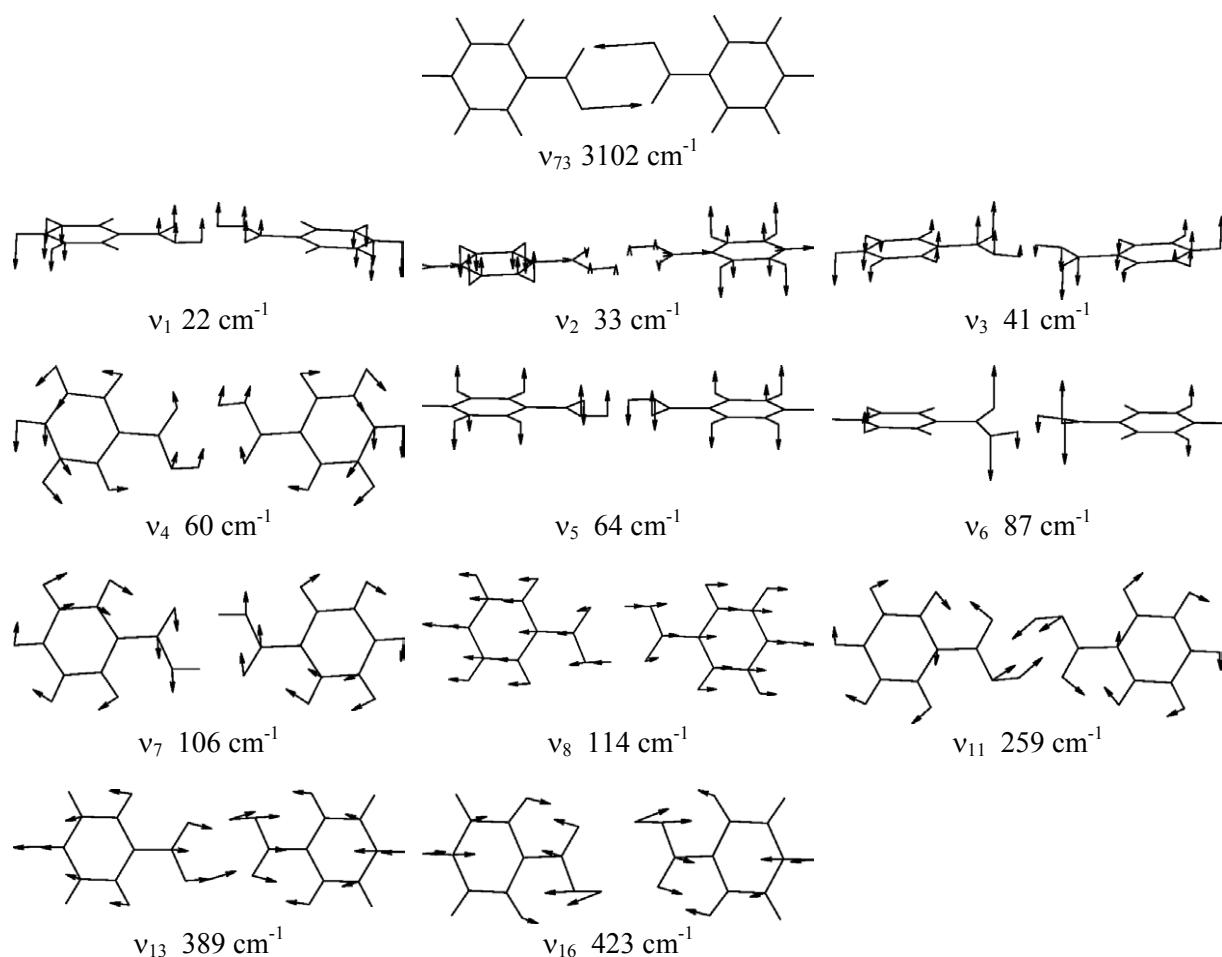
Figure 2. Normal modes of benzoic acid calculated by the B3LYP/6-311++G** method.

Table 3. Calculated energies and barrier for benzoic acid by the B3LYP/6-311++G** (DFT) method.

		DFT
Energy, stable structure	No ZPE, a.u.	-841,923
	With ZPE, a.u.	-841,691
Energy, saddle point structure	No ZPE, a.u.	-841,912
	With ZPE, a.u.	-841,688
Energy barrier	No ZPE, kcal/mol	6,497
	No ZPE, cm^{-1}	2272
	With ZPE, kcal/mol	1,867
	With ZPE, cm^{-1}	653

Model Calculations

On the basis of the *ab initio* calculations we constructed two-dimensional model PES for the proton tunnelling v_{73} coupled to chosen low-frequency modes of benzoic acid dimer which largely affect the tunnelling. These are the low-frequency planar hydrogen-bond stretching and bending modes v_4, v_7, v_8, v_{11}, v_{13} and v_{16} and the lowest-frequency out-of-plane modes v_1, v_2, v_3, v_5 and v_6. They are shown in Fig. 2 and their calculated vibrational frequencies are listed in Table 2. We assumed the symmetric (synchronous) double proton transfer in benzoic acid dimer in accordance with the results of ref. [18].

The two-dimensional model potentials used to simulate the couplings are [12,13]:

(a) the symmetric mode coupling potential (SMC) describing couplings of the proton tunnelling mode v_1 with the planar modes v_8, v_9 and v_{21}:

$$V_{SMC} = \frac{1}{8x_0^2}(x - x_0)^2(x + x_0)^2 + \frac{1}{2}\frac{\omega_y}{\omega_x}\left[y + \alpha\left(x^2 - x_0^2\right)\right]^2 \tag{1}$$

and

(b) the squeezed double well potential (SQZ) describing couplings of the proton tunneling mode v_1 with the out-of-plane modes v_{12}, v_{13} and v_{24}:

$$V_{SQZ} = \frac{1}{8x_0^2}(x - x_0)^2(x + x_0)^2 + \frac{1}{2x_0^2}\left[\frac{\omega_z}{\omega_x}x_0^2 - \gamma\left(x^2 - x_0^2\right)/\left(\frac{\omega_z}{\omega_x}\right)\right]z^2, \tag{2}$$

where x and y and z, denote the coordinates of the proton tunneling and the low-frequency modes, respectively, ω_x, ω_y and ω_z are the angular frequencies, $2x_0$ the distance between the two minima, α and γ the coupling strengths. In the formulas (1) and (2) the potentials are expressed in the units of the quantum $\hbar\omega_x$ and the coordinates x, y and z are dimensionless:

$$x = \tilde{x}\sqrt{\frac{m_x\omega_x}{\hbar}},$$

$$y = \tilde{y}\sqrt{\frac{m_y\omega_y}{\hbar}}, \tag{3}$$

$$z = \tilde{z}\sqrt{\frac{m_z\omega_z}{\hbar}}.$$

$\tilde{x}$, $\tilde{y}$ and $\tilde{z}$ denote the dimensional coordinates and m_x, m_y and m_z are the effective masses.

The parameters x_0, α and γ of the potentials (1) and (2) were estimated from the formulas:

$$\Delta E = \frac{x_0^2}{8}\hbar\omega_x,$$

$$y_s = \alpha\, x_0^2, \tag{4}$$

$$\gamma = \frac{\left(\omega_z^s - \omega_z\right)\omega_z}{\omega_x^2},$$

where ΔE, y_s and ω_z^s denote the energy barrier, the value of the normal coordinate y of the coupled mode of the SMC potential at the saddle point structure and the angular frequency of the mode z at the

saddle point structure, respectively. We used no ZPE energy barriers. The parameters used in subsequent calculations of the energy splittings have been calculated from the results of the B3LYP/6-311++G** data and are listed in Table 4. The parameter α describing coupling between the O-H stretching mode ν_{73} and the mode ν_4, ν_7, ν_8, ν_{11}, ν_{13} or ν_{16} represent an analogue of linear distortion parameters b used for theoretical reproduction of the X-H infrared band shapes of tropolone [34], salicylaldehyde [35] or aspirin [36]. Both different spectroscopic facts thus have the same origin, the anharmonic coupling in the potential energy between the two X-H and X...Y vibrations.

Tunnelling energy splittings have been calculated variationally. The convergence has been confirmed by reproducing exactly the energy splittings reported by Takada and Nakamura [12] and calculated by the DVR method [37,38]. The results are presented in Table 5 for the two-dimensional model potentials (1) and (2). The proton tunnelling energy splitting in the vibrationally ground states of the low-frequency modes is ca. 230 cm^{-1}. This compares reasonably well with the experimental value 172 cm^{-1} obtained from the inelastic neutron scattering measurements for benzoic acid - D_5H and recently reported by Fillaux et al. [30]. The two-dimensional model PES qualitatively explain increase of the tunnelling splitting with the excitation of the planar ν_4, ν_7, ν_8, ν_{11}, ν_{13} and ν_{16} modes. For the out-of-plane modes the monotonic change depend on a sign of the coupling parameter γ. When the sign is positive (for modes ν_1 and ν_2) one obtains monotonic decrease of the splitting with the excitation, and when it is negative (for the ν_3, ν_5 and ν_6 mode) the excitations cause increase of the splittings. This remains in agreement with our previous theoretical results for the excited state of tropolone [13] and hydrogen carbonate dimer [23]. Experimentally observed in tropolone promotion of the tunnelling by the excitation of the planar modes and its suppression by the excitation of the out-of-plane modes [7,8] are qualitatively confirmed in the present two-dimensional model calculations. Our previous results on the excited state of tropolone [13], hydrogen carbonate dimer ion [23] and the present ones do not require any adjustments and present pure quantum-mechanical approach to the problem of tunnelling splittings.

Table 4. Parameters of the two-dimensional models.

Mode				
Stable	Saddle point	x_o	α	γ
ν_4		2,42	0,178	
ν_7		2,42	0,096	
ν_8		2,42	0,122	
ν_{11}		2,42	0,040	
ν_{13}		2,42	0,056	
ν_{16}		2,42	0,138	
	ν_1	2,42		0,00000017
	ν_2	2,42		0,00000597
	ν_3	2,42		-0,00010000
	ν_5	2,42		-0,00000807
	ν_6	2,42		-0,00007099

Table 5. Energy splittings (cm^{-1}) calculated for two-dimensional model potentials.

Quantum number	SMC						SQZ				
	ν_4	ν_7	ν_8	ν_{11}	ν_{13}	ν_{16}	ν_1	ν_2	ν_3	ν_5	ν_6
0	229,24	229,50	229,36	229,67	229,65	229,54	229,71	229,63	230,99	229,78	230,10
1	229,43	229,68	229,69	229,86	230,52	235,50	229,71	229,47	233,54	229,89	230,87
2	229,62	229,86	230,02	230,05	231,38	241,32	229,70	229,30	236,12	230,01	231,64
3	229,82	230,04	230,35	230,25	232,23	247,01	229,69	229,14	238,74	230,13	232,41
4	230,01	230,22	230,68	230,44	233,09	252,57	229,69	228,97	241,39	230,25	233,18
5	230,20	230,40	231,01	230,63	233,94	258,02	229,68	228,81	244,08	230,37	233,96
6	230,39	230,57	231,34	230,82	234,79	263,36	229,67	228,64	246,80	230,49	234,74
7	230,58	230,75	231,67	231,02	235,63	268,59	229,66	228,48	249,55	230,60	235,52
8	230,77	230,93	231,99	231,21	236,48	273,72	229,66	228,31	252,34	230,72	236,30
9	230,96	231,11	232,32	231,40	237,31	278,76	229,65	228,15	255,16	230,84	237,09
10	231,15	231,29	232,65	231,59	238,15	283,70	229,64	227,98	258,01	230,96	237,88

Conclusions

The proton tunnelling dynamics in benzoic acid dimer in the ground electronic state has been studied by performing quantum mechanical calculations of the potential energy surface and fitting it by two-dimensional model potentials. The tunnelling energy splittings for different vibrationally excited states have been calculated. The calculated proton tunnelling energy splitting in the vibrationally ground states of the low-frequency modes (~230 cm^{-1}) compares reasonably well with the experimental value 172 cm^{-1} obtained from the inelastic neutron scattering measurements for benzoic acid - D$_5$H [29]. Our model calculations predict the promotion of the proton tunnelling by the excitation of the planar modes. Depending of the sign of the coupling parameter γ, out-of-plane modes can either supress or promote the tunnelling. This results are confirmed by existing experimental data [7,8]. Our model presents a pure quantum-mechanical approach to the problem of the proton tunnelling splittings.

References

1. Löwdin, P.O. *Rev. Mod. Phys.* **1963**, *35*, 724.
2. Nakamura, H. *Ann. Rev. Phys. Chem.* **1997**, *48*, 299.
3. Alves, A.C.P.; Hollas, J.M. *Mol. Phys.* **1973**, *25*, 1305.
4. Redington, R.L; Redington, T.E. *J. Mol. Spectr.* **1979**, *78*, 229.
5. Tomioka, Y.; Ito, M.; Mikami, N. *J. Phys. Chem.* **1983**, *87*, 4401.
6. Redington, R.L.; Chen, Y.; Scherer, G.J; Field, R.W. *J. Chem. Phys.* **1988**, *88*, 627.
7. Sekiya, H.; Nagashima, Y.; Nishimura, Y. *J. Chem. Phys.* **1990**, *92*, 5761.
8. Sekiya, H.; Nagashima, Y.; Tsuji, T.; Nishimura, Y.; Mori, A.; Takeshita, H. *J. Phys. Chem.* **1991**,

95, 10311.

9. Nishi, K.; Sekiya, H.; Kawakami, H.; Mori, A.; Nishimura, Y. *J. Chem. Phys.* **1998**, *109*, 1589.

10. Vener, M.V.; Scheiner, S.; Sokolov, N.D. *J. Chem. Phys.* **1994**, *101*, 9755.

11. Smedarchina, Z.; Siebrand, W.; Zgierski, M.Z. *J. Chem. Phys.* **1996**, *104*, 1203.

12. Takada, S.; Nakamura, H. *J. Chem. Phys.* **1995**, *102*, 3977.

13. Wójcik, M.J.; Nakamura, H.; Iwata, S.; Tatara, W. *J. Chem. Phys.* **2000**, *112*, 6322.

14. Carrington, T. Jr.; Miller, W.H. *J. Chem. Phys.* **1986**, *84*, 4364.

15. Shida, N.; Barbara, P.F.; Almlof, J.E. *J. Chem. Phys.* **1989**, *91*, 4061.

16. Smedarchina, Z.; Siebrand, W.; Zgierski, M.Z. *J. Chem. Phys.* **1995**, *103*, 5326.

17. Sewell, T.D.; Guo, Y.; Thompson, D.L. *J. Chem. Phys.* **1995**, *103*, 8557.

18. Shida, N.; Barbara, P.; Almlof, J.E. *J. Chem. Phys.* **1991**, *94*, 3633.

19. Nishi, K.; Sekiya, H.; Kawakami, H.; Mori, A.; Nishimura, Y. *J. Chem. Phys.* **1998**, *109*, 1589.

20. Nishi, K.; Sekiya, H.; Kawakami, H.; Mori, A.; Nishimura, Y. *J. Chem. Phys.* **1999**, *111*, 3961.

21. Nishi, K.; Sekiya, H.; Mochida, T.; Sugawara, T.; Nishimura, Y. *J. Chem. Phys.* **2000**, *112*, 5002.

22. Vener, M.V.; Sauer, J. *J. Chem. Phys.* **2001**, *114*, 2623.

23. Wójcik, M.J.; Tatara, W.; Ikeda, S. *J. Mol. Struct.* **2002**, *614*, 109.

24. Decornez, M.; Drukker. H.; Hammes-Schiffer, S. *J. Phys. Chem. A* **1999**, *103*, 2891.

25. Mavri, S.; Grdadolnik, J. *J. Phys. Chem. A* **2001**, *105*, 2045.

26. Sim, G.A.; Monteath Robertson, J.; Goodwin, T.H. *Acta Cryst.* **1955**, *8*, 157.

27. Wilson, C.C.; Shanklandnd.N.; Florence, A.J. *Chem. Phys. Lett.* **1996**, *253*, 103.

28. Bruno, G.; Randaccio, L. *Acta Cryst.* **1980**, *B36*, 1711.

29. Plazanet, M.; Fukushima, N.; Johnson, M.R.; Horsewill, A.J.; Trommsdorf, H.P. *J. Chem. Phys.* **2001**, *115*, 3241.

30. Fillaux, F.; Limage, M.H.; Romain, F. *Chem. Phys.* **2002**, *276*, 181.

31. Stepanian, S.G; Reva, I.D; Radchenko, E.D.; Sheina, G.G., *Vibrat. Spectrosc.* **1996**, *11*, 123.

32. Zelsmann, H.R; Mielke, Z. *Chem. Phys. Lett.* **1991**, *186*, 501.

33. Frisch, M.J.; Trucks, G.W; Schlegel, H.B.; Scuseria, G.E.; Robb, M.A.; Cheeseman, J.R.; Zakrzewski, V.G.; Montgomery, J.A., Jr., Stratmann, R.E.; Burant, J.C.; Dapprich, S.; Millam, J.M.; Daniels, A.D.; Kudin, K.N.; Strain, M.C.;Farkas, O.; Tomasi, J.; Barone, V.; Cossi, M.; Cammi, R.; Mennucci, B.; Pomelli, C.; Adamo, C.; Clifford, S.; Ochterski, J.; Petersson, G.A.; Ayala, P.Y.; Cui, Q.; Morokuma, K.; Malick, D.K.; Rabuck, A.D.; Raghavachari, K.; Foresman, J.B.; Cioslowski, J.; Ortiz, J.V.; Stefanov, B.B.; Liu, G.; Liashenko, A.; Piskorz, P.; Komaromi, I.; Gomperts, R.; Martin, R.L.; Fox, D.J.; Keith, T.; Al-Laham, M.A.; Peng, C.Y.; Nanayakkara, A.; Gonzalez, C.; Challacombe, M.; Gill, W.; Johnson, B.; Chen, W.; Wong, M.W.; Andres, J.L.; Gonzalez, C.; Head-Gordon, M.; Replogle, E.S.; Pople, J.A. Gaussian 98, Revision A.6; Gaussian: Pittsburgh PA, 1998.

34. Wójcik, M.J; Boczar, M.; Stoma, M. *Int. J. Quant. Chem.* **1999**, *73*, 275.

35. Boczar, M.; Wójcik, J.M; Szczeponek, K.; Jamróz, D; Ikeda, S. *Int. J. Quant. Chem.* **2002**, *90*, 689.

36. Boczar, M.; Wójcik,M.J; Szczeponek, K; Jamróz, D.; Zięba A.; Kawałek, B. *Chem. Phys.* **2002**, *286*, 63.

37. Light, J.C.; Hamilton, I.P.; Lill, J.V. *J. Chem. Phys.* **1985**, *82*, 1400.
38. Whitnell, R.M; Light, J.C. *J. Chem. Phys.* **1989**, *90*, 1774.